BB-3

MEASUREMENTS AND MODELING OF KINETIC INDUCTANCE MICROSTRIP DELAY LINES

J. M. Pond, J. H. Claassen, and W. L. Carter

Naval Research Laboratory, Washington, DC 20375

ABSTRACT

Microstrip, with phase velocities of about 0.01c, employing kinetic inductance have been fabricated using niobium nitride and a silicon dielectric. Delay lines employing the phenomenon of kinetic inductance have several advantages for analog signal processing, including low loss and very compact size. An analysis of kinetic inductance microstrip delay lines has been made in the frequency domain and the time domain. The results were compared to theoretical predictions and an accurate circuit model was developed.

INTRODUCTION

There has been substantial work involving the use of superconducting microstrip and stripline to accomplish delay and other signal processing applications (1,2). By using conventional microstrip or stripline geometry, where the conductors are replaced by superconductors, performance surpassing conventional techniques has been obtained. This delay line technology has low loss due to the superconductor and hence a higher frequency capability than other approaches.

Recently it has been reported (3) that additional performance advantages can result by exploiting the effects of kinetic inductance (L_k). L_k is due to the inertial mass of the current carriers in a conductor. The difficulty in observing L_k in a normal wire is evident by considering that the resistance per unit length of a conductor of cross sectional area A is given by

$$R = m/(ne^2)(1/A)(1/\tau). \qquad \text{Eq. 1}$$

At a radian frequency ω, the kinetic reactance per unit length, in simplest form, is given by

$$\omega L_k = m/(ne^2)(1/A)\omega, \qquad \text{Eq. 2}$$

where m, n, e and τ are the mass, density, charge and collision time of an electron. Only if the conductor is superconducting ($\tau \to \infty$) is $\omega > 1/\tau$ for frequencies in the microwave regime and hence the kinetic reactance dominates the resistance. Under normal geometries, even with a superconductor, the magnetic inductance (L_m) is several orders of magnitude greater than the L_k contribution.

The slowing of an electromagnetic wave on a superconducting transmission line due to the contribution of L_k was pointed out by Pippard in 1947 (4). The measurement of this slowing, using thin films, has been exploited as a method of determining the penetration depth of thin superconducting films (5). Solutions to the electromagnetic boundary value problem for a trilayer of a thin superconducting film, a lossy dielectric and a thin superconducting film have been presented using Maxwell's equations for both the simple two fluid model (6) and the Mattis-Bardeen theory for complex conductivity (7).

In addition, this technology has the unique capability of continuously varying the phase velocity over at least a 2:1 range, by varying the relative populations of the superconducting and normal electrons. This concept is applicable to making microstrip phase shifters and tunable filters as well as variable delay lines.

NUMERICAL CALCULATIONS

In attempting to exploit L_k for microwave delay lines, the circumstances which give rise to the slowest possible phase velocity with minimum loss and dispersion are of interest. It is assumed that the dielectric thickness (d) and the penetration depth (λ) are small compared to the wavelength and to the length of the microstrip line. If it is further assumed that the width (w) of the microstrip line is small compared to a wavelength and to d, then, using either model mentioned above, the phase velocity is given as

$$v_p = c[\varepsilon_r(1 + (\lambda_1/d)\coth(t_1/\lambda_1) + (\lambda_2/d)\coth(t_2/\lambda_2))]^{-1/2} \qquad \text{Eq. 3}$$

where c is the speed of light in vacuum. It can be seen that to minimize the phase velocity it is desirable to have $d \ll \lambda_1$, $d \ll \lambda_2$, $t_1 \ll \lambda_1$ and $t_2 \ll \lambda_2$. This is limited in practice by the difficulty of obtaining a very thin dielectric which is free of pin holes and has low losses.

The velocity given by Eq. 3 can be compared with the expression in terms of capacitance per unit length (C) and inductance per unit length (L) where,

$$v_p = (LC)^{-1/2}. \qquad \text{Eq. 4}$$

Since the C is given by the parallel plate expression then L is given by

$$L = \mu_o d[1 + (\lambda_1/d)\coth(t_1/\lambda_1) + (\lambda_2/d)\coth(t_2/\lambda_2)]/w \qquad \text{Eq. 5}$$

assuming ε_o and μ_o are the permittivity and permeability of free space and ε_r is the relative permittivity. The first term is due to L_m and the second and third terms are due to L_k of the top and bottom thin superconducting metal layers.

Expressions exist for the group velocity and the frequency dependent losses of the superconductors (6,7). With the exception of frequencies near the gap frequency, it has been shown that the difference between the two-fluid model and the Mattis-Bardeen model is minimal (8). As has been shown (3) , dielectric loss of the microstrip under consideration is the dominant attenuation in the line and for this reason the simpler two fluid model is used for the following calculations. It is assumed that the penetration depth follows a dependence given by

$$\lambda = \lambda_o[1-(T/T_c)^4\ ]^{-1/2} \qquad \text{Eq. 6}$$

where T_c is the critical temperature and λ_o is the penetration depth at 0.0 K.

The dielectric losses are given by

$$\alpha_d = (\omega/2v_p\ )(\varepsilon''/\varepsilon') \qquad \text{Eq. 7}$$

where ε' and ε'' are the real and imaginary parts of the permittivity, and would dominate the superconductor losses at 2.0 GHz for $\varepsilon''/\varepsilon'$ as low as 10^{-7}. Deposited films usually have substantially higher values of $\varepsilon''/\varepsilon'$.

In the regime where $L_k \gg L_m$ and $t \ll \lambda$ and assuming that $t_1 = t_2 = t$ and $\lambda_1 = \lambda_2 = \lambda$, the expressions for v_p and Z_o can be simplified as

$$Z_o = \lambda/w \left[\frac{2d\,\mu_o}{\varepsilon_o \varepsilon_r t} \right]^{1/2} \qquad \text{Eq. 8}$$

and

$$v_p = 1/\lambda \left[\frac{dt}{2\,\mu_o \varepsilon_o \varepsilon_r} \right]^{1/2} . \qquad \text{Eq. 9}$$

From these equations it is possible to construct a wide variety of design curves for practical situations which show the functional dependence of the velocity and impedance of a microstrip line as a function of the geometry. In all most all cases w is at least an order of magnitude larger than d and hence the use of equations developed from the parallel plate analysis are valid.

The dependence of v_p, normalized to c and $c/\sqrt{\varepsilon_r}$, and Z_o as a function of t for several values of w (in μm) is plotted in Fig. 1. It is assumed that d = 100 nm, λ = 300 nm and ε_r = 12. The slowing factor due to L_k varies from less than 0.04 to greater than 0.20 as t is decreased. For t in the range of about 10 nm to 20 nm very practical values for Z_o can be obtained using high quality optical lithography. This fact is relevant to the design of tunable filters. The tunability is a consequence of the dependence of λ on the relative populations of the superconducting to normal electrons. This is most easily varied by adjusting temperature as indicated in Eq. 6, but can also be accomplished optically and possibly electronically.

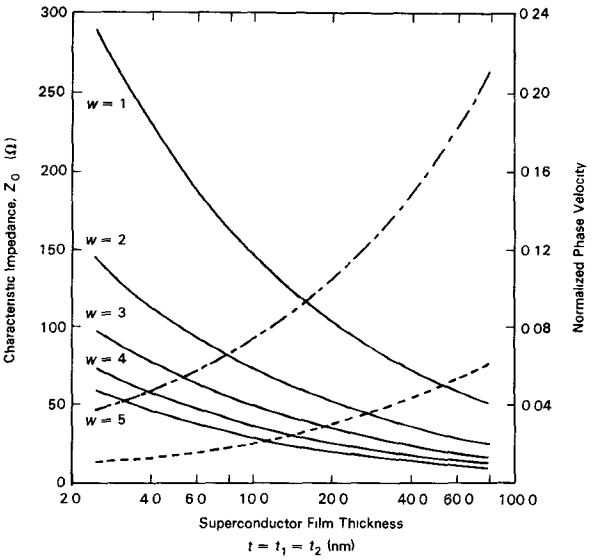

Fig. 1 Z_o (——), v_p/c (- - -) and $\sqrt{\varepsilon_r} v_p/c$ (- —— -) versus t for several w (in μm) with d = 100 nm, λ = 300 nm and ε_r = 12.0

DEVICE FABRICATION AND TEST FIXTURE

The devices were fabricated in an ultra high vacuum RF sputtering system. For the particular sample to be discussed in the remainder of the paper, a 150 Å NbN ground plane was deposited on a quartz substrate followed by 250 Å of hydrogenated silicon (Si:H). In order to avoid shorts, these layers were patterned and plasma etched to open holes in the ground plane for the microstrip contact pads. Then, 150 Å of Si:H was deposited followed by a second NbN layer of 140 Å.

Contact pads were then patterned which were connected by a 25 μm wide 20.1 cm long microstrip. The contact pads were then covered by 100 Å of Cr and 1000 Å of Au. It was found that in order to have a repeatable contact it was necessary to melt some indium on the Au contacts.

The sample was mounted in a fixture which used 0.141 inch coaxial cable with a spring loaded center conductor to contact the contact pads perpendicular to the substrate surface. The test fixture was then mounted in a cryostat with 110 cm coaxial cable feedthroughs to room temperature.

EXPERIMENTAL RESULTS

Frequency responses were made using Hewlett Packard 8409 and 8510 automatic network analyzers. The power incident on the device was set at 100 μW and the scattering matrix of the delay line and the feedthrough cables was measured in 50 MHz and 100 MHz frequency bands around 0.1 GHz, 0.5 GHz, 1.0 GHz and 2.0 GHz in 1.0 MHz increments. These measurements were made at 4.2 K, 7.3 K and 9.0 K. Fig. 2 shows representative data for the magnitude of the transmission coefficients for the delay

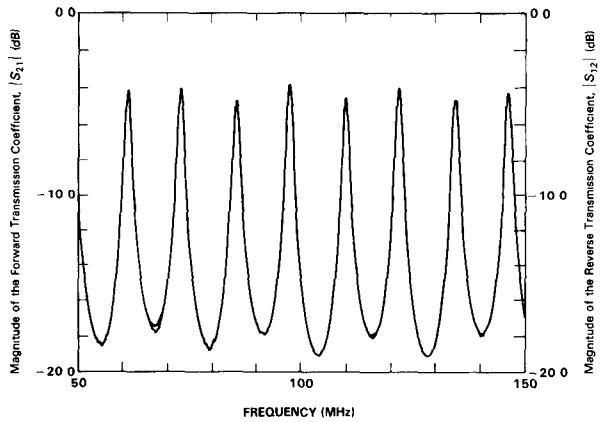

Fig. 2 Magnitude of the transmission response of the delay line at 4.2 K.

line and test fixture. The sharp peaks of $|S_{21}|$ correspond to frequencies where the delay line is an integral number of half wavelengths long. This is due to the large impedance mismatch and discontinuity which causes the delay line to appear as a weakly coupled cavity with an input and output port. Thus

$$v_p = 2 \ell \Delta f \qquad \text{Eq. 10}$$

where ℓ is the length of the line and Δf is the separation between peaks in $|S_{21}|$. Similar measurements were obtained at other frequencies and temperatures and the resonant peaks remained well defined up to at least 2.0 GHz .

The time domain response of the line is shown in Fig. 4. This data was obtained using the time domain function of the HP 8510 and a frequency band of 0.05 GHz to 0.50 GHz. These measurements agree very well with transient measurements made using a pulse generator (3). Due to the large discontinuity most of the incident pulse is reflected and the transmitted pulse is reflected many times within the delay line. At each reflection some of the power is transmitted out of the delay line and into the coax. The pulses are undistorted with a spacing that corresponds to the double transit time of the line.

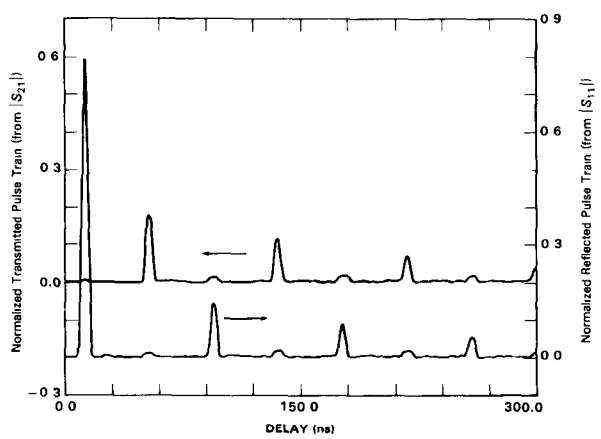

Fig. 3 Reflected and transmitted time domain response for the delay line.

The measured temperature dependencies of v_p and α, assuming lossless discontinuities, are shown in Fig. 4. The temperature dependence is as expected from Eq. 7. An absolute comparison is not possible since a separate measurement of λ_o was not available, however the results are consistent with $\lambda_o \simeq 300$ nm. This is a reasonable number for thin films of NbN.

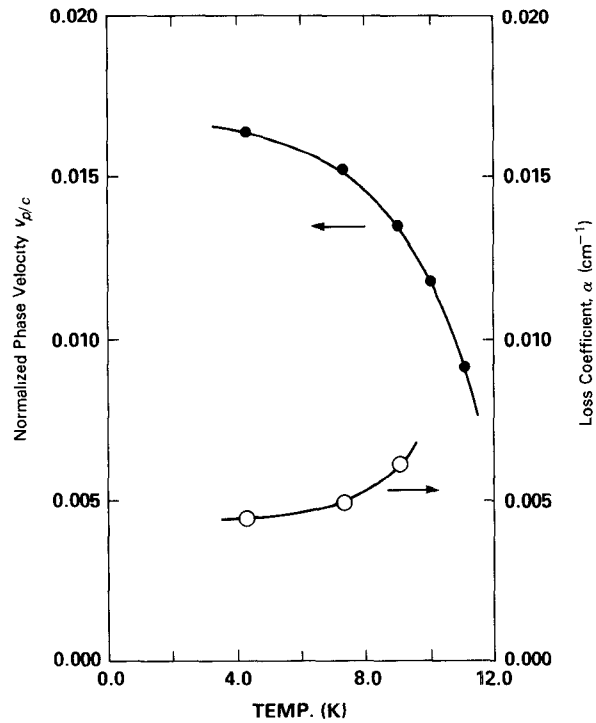

Fig. 4 v_p and α versus temperature at 0.1 MHz.

MODELING

Modeling of this microwave circuit was done using EEsof's Touchstone program. Examination of Fig. 3 indicates an interesting signature in the frequency response. The minima in the response show a peiodicity in amplitude which is twice the period of the structure. The amplitude variations in the maxima are not real but due to the discretization of the frequency measurement.

This same phenomenon can be seen in the time domain response of Fig. 4 where small pulses can be seen half way between the major pulses of both the reflected and transmitted pulse train. This signature is attributed to a parallel conduction path through the substrate. This can occur since the "ground plane" of the microstrip is not actually at ground potential but is connected to ground through the superconducting film which has an associated kinetic inductance. Confirmation of this hypothesis was obtained by measuring a control device in which the delay line was not connected. Fig. 5 shows the forward and reverse pulses due to the parallel conduction path.

The equivalent circuit is shown in Fig. 6. The delay line is modeled by a floating transmission line which is 20.1 cm long. The slow

velocity was simulated by choosing a very large effective dielectric value. The loss of the delay line at this frequency is 0.50 dB/cm assuming that the transitions are lossless. The loss of the input and output coaxial lines was accounted for with measured values. A comparison of this model with the measured response is shown in Fig. 7 where it can be seen that the model agrees very well with the data. The model, however, does not fit the data as accurately broadband but does closely reproduce the data and an equivalent fit can be obtained with small changes in the values of C_1, L_1 and Z_1.

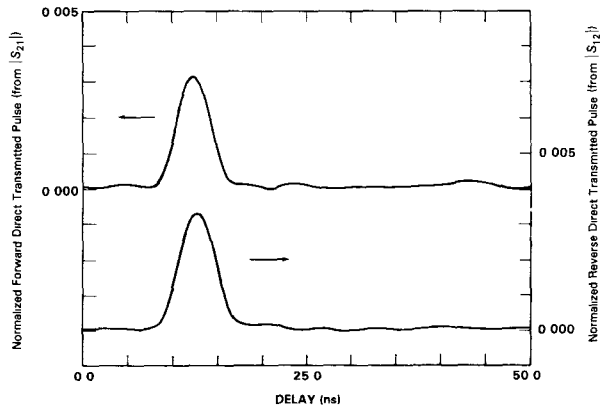

Fig. 5 Direct transmitted pulses due to the parallel transmission path through the substrate.

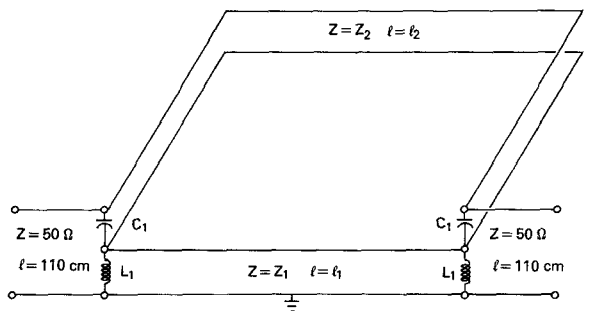

Fig. 6 Equivalent circuit which accurately models the device response.

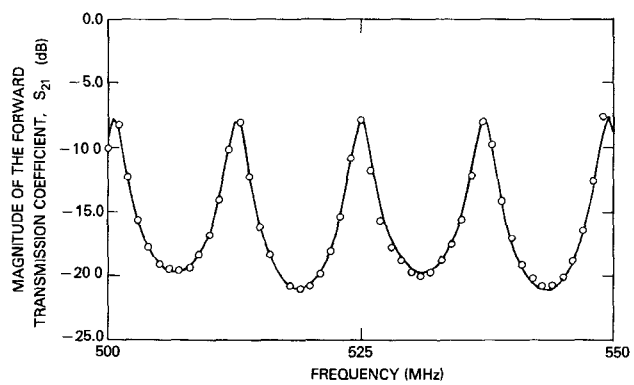

Fig. 5 Comparison of the equivalent circuit response (——) and measured response (o) with Z_1 = 25 Ω, ℓ_1 = 1.0 cm, C_1 = 1.0 pF, and a line loss in the device of 0.05 dB/cm.

CONCLUSIONS

The particular advantage of this technique is the possibility of obtaining very large variable delays in a very small area due to the reduced velocity and small coupling between lines. In addition these devices have the potential for high frequency operation. These devices can be described and hence designed by common computer aided design systems. Due to the processing compatibility with Josephson and tunnel junction technology, this technology allows the possibility of accomplishing sophisticated signal processing functions as well as combined analog and digital functions. The primary area of emphasis for future work will be in the implementation of other devices such as phase shifters, tunable filters, taps and coupled lines. Obtaining accurate and repeatable control of the velocity is important for this technology.

ACKNOWLEDGEMENTS

The authors would like to acknowledge the helpful discussions of Drs. Denis Webb, Martin Nisenoff and Edward Cukauskas. This work was supported by the Office of Naval Research.

REFERENCES

(1) D. A. Gandolfo, A. Boornard, and L. C. Morris, "Superconductive microwave meander lines", J. Appl. Phys., 39, 2657-2660, 1968.

(2) S. A. Reible, "Wideband analog signal processing with superconductive circuits", 1982 IEEE Ultrasonics Symnposium Digest, 190-201.

(3) J. M. Pond, J. H. Claassen, and W. L. Carter, "Kinetic inductance microstrip delay lines", accepted in IEEE Trans. Mag., Spring, 1987.

(4) A. B. Pippard, "The surface impedance of super conductor and normal metals at high frequencies, III The relationship between impedance and superconducting penetration depth ", Proc. Roy. Soc. Lond., A191, 399-415, 1947.

(5) W. H. Henkels, and C. J. Kircher, "Penetration depth measurements on type II superconducting films", IEEE Trans. Mag., MAG-13, No. 1, 1977.

(6) J. C. Swihart, "Field solution for a thin-film superconducting strip transmission line", J. Appl. Phys., 32, 461-469, 1961.

(7) P. V. Mason, and R. W. Gould, "Slow-wave structures utilizing superconducting thin film transmission lines", J. Appl. Phys., 40, 2039-2051, 1969.

(8) R. L. Kautz, "Picosecond pulses on superconducting striplines", J. Appl. Phys., 49, 308-314, 1978.